

RESEARCH

Open Access



Quantitative assessment of ECRB tendon degeneration in lateral epicondylitis using CT hounsfield units: correlation with histological and MRI findings

Shigeki Ishibashi¹, Akira Kodama^{1,2*}, Maya Tokumoto¹, Kazushi Yokomachi³, Rikuo Shinomiya^{1,4} and Nobuo Adachi¹

Abstract

Background Lateral epicondylitis (LE) is characterized by enthesopathy and tendon degeneration of the extensor carpi radialis brevis (ECRB) attachment. Although magnetic resonance imaging (MRI) can reveal pathological changes, quantitative evaluation methods remain limited. This study aimed to quantify ECRB tendon degeneration on computed tomography (CT) using Hounsfield unit (HU) values.

Methods We analyzed 24 elbows (12 males, 12 females; mean age: 53.7 years) in the LE group and 25 control elbows (16 males and 9 females; mean age: 56.7 years). All the patients in the study group underwent preoperative CT, MRI, and subsequent ECRB tendon resection. The tendon was divided into proximal, middle, and distal regions. The mean HU values were measured on reconstructed coronal CT images and analyzed in relation to the control group measurements, MRI findings, and histological evaluations.

Results The mean HU values were significantly lower in the LE group than in the controls in the proximal (49.7 vs. 65.4 HU, $P < .0001$) and middle regions (58.9 vs. 67.1 HU, $P = 0.024$) but not in the distal region (66.1 vs. 70.8 HU, $P = 0.192$). The ECRB tendon showed the greatest histological degeneration proximally, demonstrating a strong negative correlation with HU values (Spearman $\rho = -0.612$, $P < .0001$). Proximal region HU values showed a moderate negative correlation with MRI grades (Spearman $\rho = -0.517$, $P = 0.020$).

Conclusion HU values provide a quantitative method for evaluating ECRB tendon degeneration in LE, correlating well with histological and MRI findings. This technique offers an objective measure of tendon pathology that may complement the current diagnostic approaches.

Evidence from the study Level III.

Keywords Lateral epicondylitis, Computed tomography, Hounsfield unit, Extensor carpi radialis brevis, Magnetic resonance imaging, Quantitative assessment, Tendon degeneration

*Correspondence:

Akira Kodama
akirakodama@hiroshima-u.ac.jp

Full list of author information is available at the end of the article



© The Author(s) 2025. **Open Access** This article is licensed under a Creative Commons Attribution-NonCommercial-NoDerivatives 4.0 International License, which permits any non-commercial use, sharing, distribution and reproduction in any medium or format, as long as you give appropriate credit to the original author(s) and the source, provide a link to the Creative Commons licence, and indicate if you modified the licensed material. You do not have permission under this licence to share adapted material derived from this article or parts of it. The images or other third party material in this article are included in the article's Creative Commons licence, unless indicated otherwise in a credit line to the material. If material is not included in the article's Creative Commons licence and your intended use is not permitted by statutory regulation or exceeds the permitted use, you will need to obtain permission directly from the copyright holder. To view a copy of this licence, visit <http://creativecommons.org/licenses/by-nc-nd/4.0/>.

Introduction

Lateral epicondylitis (LE) is common in clinical practice. LE is diagnosed based on clinical history and physical examination, and the criteria for surgery and treatment efficacy are based on subjective evaluation [1]. Most patients benefit from conservative treatment, but surgical treatment is indicated if symptoms do not improve after 3–6 months of conventional treatment [2].

The pathogenesis of LE is mainly enthesopathy due to tendon degeneration and fiber tears at the extensor carpi radialis brevis (ECRB) attachment [3–5]. Magnetic resonance imaging (MRI) has been used to evaluate tendon attachments, with T2-weighted images showing hyperintense changes [6–9]. While specialized MRI techniques such as T2/T2* mapping can provide quantitative assessment of tendons and ligaments when specific scanning protocols are used. These methods have limitations in evaluating histological changes [10]. Quantitative evaluation may help determine the treatment effectiveness, disease severity, surgical indications, and extent of ECRB curettage required during surgery. Additional quantitative methods could potentially complement existing imaging techniques for assessing these clinical parameters.

Computed tomography (CT) images enable the quantitative evaluation of soft tissues using Hounsfield unit (HU) values, a standardized scale for radiographic density. This scale ranges from –1000 for air through 0 for water to +1000 for calcified tissue [11]. It is a value proportional to the X-ray absorption coefficient based on the scale. CT is not only excellent for delineating the calcification of the cortical bone and soft tissues, but is also used for soft tissue evaluation. Measurement of HU values has been used to diagnose acute stroke [12] and fatty liver [13] and to evaluate fatty infiltration in muscles [14]. Recent reports have indicated that hypodense degenerative changes in tendons and ligaments, such as the Achilles tendon [15], posterior cruciate ligament of the knee [16], and deltoid ligament [17], can be evaluated. We hypothesized that ECRB tendon degeneration in LE can be quantified using HU values. This study aimed to examine the relationship between the HU values of the tendon and both histopathological and MRI findings to validate this hypothesis. Furthermore, we compared these HU values with those obtained from CT scans of healthy individuals to gain insight into their significance in the context of LE.

Materials and methods

This study was approved by the ethics committee of the authors' institution (approval no.: E2022-0252) and conducted in accordance with the Declaration of Helsinki. All participants signed a written informed consent form

approved by the review committee after being informed about the CT, MRI, and histological study.

This prospective observational study included consecutive patients who underwent surgery for LE between Jul 2015 and Jan 2023. All patients underwent preoperative CT and MRI followed by ECRB tendon resection during surgery. Independent observers, blinded to the clinical findings and other results, separately evaluated the CT, MRI, and histology. LE was defined as the most intense tenderness at the extensor tendon origin of the lateral epicondyle and pain in the lateral elbow with resistive wrist dorsiflexion exercises. Patients with disorders other than those of extensor tendon origin, such as brachiocephalic joint disorders, and those suspected of having radial tunnel syndrome were excluded. Surgery was indicated for cases in which the pain persisted for >6 months despite conservative treatment. The control group was comprised of patients who underwent CT of the elbow joint at our clinic between 2018 and 2022 and exhibited no symptoms related to the lateral elbow joint, matched according to age.

Measurement of HU values

All elbows underwent preoperative CT using a 320-slice CT scanner (Aquilion ONE; Canon Medical Systems, Otawara-shi, Japan). The scanning parameters included a 512×512 matrix, a 0-degree gantry tilt, 1.25-mm prospective slice thickness, 120 kV (peak), and 100–350 mA. Two-dimensional images were generated with a 20-cm volume, 1.25-mm retrospective slice thickness, and 0.63-mm overlap.

Imaging was performed with the patient in the supine position, shoulders elevated, elbows fully extended, and forearms pronated. Images were analyzed using a Synapse Vincent Ver. 4.6.0001 (Fujifilm, Tokyo, Japan). The ECRB tendon was identified by tracing its course from the origin at the most distal anterior part of the lateral epicondyle to its insertion at the base of the third metacarpal, and coronal images were reconstructed centered on the humeral origin of the ECRB [18]. The ECRB tendon was divided into three regions (proximal, middle, and distal) from its humeral origin to the level corresponding to the midpoint of the radial head. The mean HU value was calculated for each region. HU values were measured using a polygonal ROI that included all regions shown in Fig. 1, excluding the enthesis at the origin. HU values are expressed as the mean of the regions. In cases of calcification, the area was defined as the area excluding the calcification. All measurements were performed using soft tissue filter images. Measurements were performed twice, with a gap of more than three months between sessions, by reconstructing the images to assess intra-observer reliability. Mean HU values were calculated using these measurements. HU measurements were

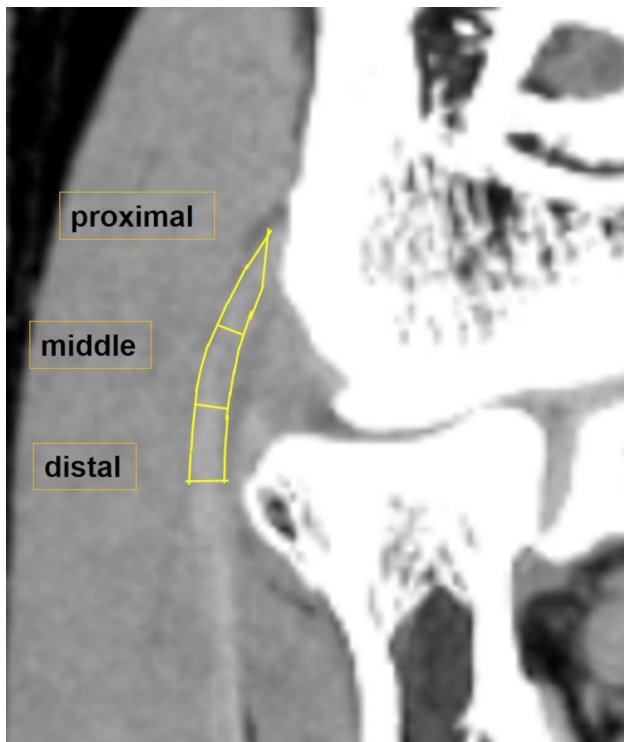


Fig. 1 Coronal image of the ECRB. The ECRB was divided into distal, middle, and proximal regions. The average Hounsfield unit (HU) value for each region was measured

performed by S.I. (an orthopaedic surgeon with over 10 years of experience and a doctoral degree) who was blinded to the clinical findings, MRI results, and histological data.

Evaluation with MRI

A 3-Tesla MRI scanner with a dedicated surface coil was used. Imaging was performed with the patient in the supine position, with the elbow fully extended, shoulder elevated, and forearm in the pronated position. A fat-suppressed T2-weighted FSE sequence was used in this study (field of view, 120–140 × 120–140 mm; matrix, 320 × 192; number of excitations, 2.0; slice thickness, 2 mm), which is considered suitable for the evaluation of tendon lesions, such as tendon rupture and tendinopathy. Based on previous studies [2, 7, 9, 19, 20], the tear thickness of the common extensor tendon (CET) was measured comprehensively using coronal and axial slices. Each was classified into four grades: grade 0, no signal change; grade 1, <20%; grade 2, 20–80%; and grade 3, >80%.

Histological evaluation

During surgery, after intra-articular evaluation using an arthroscope, an approximately 3-cm incision was made on the lateral side of the elbow joint according to Nirschl's method [21]. The extensor carpi radialis longus

was elevated above the lateral epicondyle to expose the ECRB degenerative area. The degenerative area was resected as a spindle-shaped specimen (average dimensions at its widest part: 17.6 mm in length, 5.2 mm in width, and 6.5 mm in depth) from the lateral epicondyle attachment to the proximal half of the radial head, including the articular capsule, and was evaluated as a pathological specimen. The specimens were fixed in 4% paraformaldehyde in phosphate-buffered saline (Wako Pure Chemical Industries Ltd., Osaka, Japan). After 24 h, the samples were embedded in paraffin and sectioned into 4- μ m-thick sections along the long axis using a microtome. The sections were stained with Safranin-O Fast Green and evaluated using a digital microscope (BZ-9000; Keyence, Osaka, Japan). Each specimen was examined by an expert (M.T.) with 14 years of experience in orthopaedic and histological evaluation, who was blinded to the imaging and surgical findings. Referring to the methods described in previous studies [22], the samples were divided into three regions (proximal, middle, and distal) in the same region as the imaging evaluation. Each sample was evaluated for collagen fiber damage at 40 \times magnification in ten fields of view. Grade 1 indicated poor histological changes (aligned collagen fibers, absence of fatty infiltration, or capillary proliferation), grade 2 indicated mild tendon damage, and grade 3 indicated moderate-to-severe tendon damage (loosening and degeneration of collagen fiber bonds, loss of structure, and necrosis).

Statistical analysis

All data are expressed as means and 95% confidence intervals. Patient parameters in the LE and control groups were assessed using the Mann-Whitney U test (age, body mass index [BMI]) or Fisher's exact test (sex, affected side). The HU values for the LE and control groups were evaluated using the Mann-Whitney U test. The correlation strength of HU values with MRI grade and histological grade was evaluated using Spearman's nonparametric correlation coefficient: absolute ρ values of 0–0.19, 0.2–0.39, 0.40–0.59, 0.6–0.79, and 0.8–1 were regarded as very weak, weak, moderate, strong, and very strong, respectively. Intra-observer reliability of HU measurements was assessed using intraclass correlation coefficients (ICC). The ICC values were interpreted as follows: less than 0.40, poor agreement; 0.40 and 0.75, fair to good agreement; greater than 0.75, excellent agreement. Statistical analysis was conducted using SPSS Statistics for Windows (version 22.0; IBM Corp., Armonk, NY, USA), with $P < .05$ being deemed as significant.

HU values within the LE group were compared among histological grades using the Steel-Dwass test, with $P < .05$ being deemed as significant. Nonparametric multiple comparisons for all pairs were conducted using

Table 1 Demographics of the control and LE groups

	Control (n=25)	LE (n=24)	p Value
Age at surgery, y, mean(range)	56.76 (25–77)	53.71 (37–83)	$p=0.180$
Sex, n			$p=0.393$
Men	16	12	
Women	9	12	
Side, n			$p=0.769$
Right	17	15	
Left	8	9	
Disease duration, months		10.33 (5–24)	
Body mass index	23.2 (21.8, 24.6)	24.5(22.4, 26.5)	$p=0.580$

Statistical analyses were performed for the control and LE groups. Age and disease duration are presented as mean (range). Body mass index (BMI) is presented as the mean and 95% confidence interval

Abbreviations: LE, lateral epicondylitis

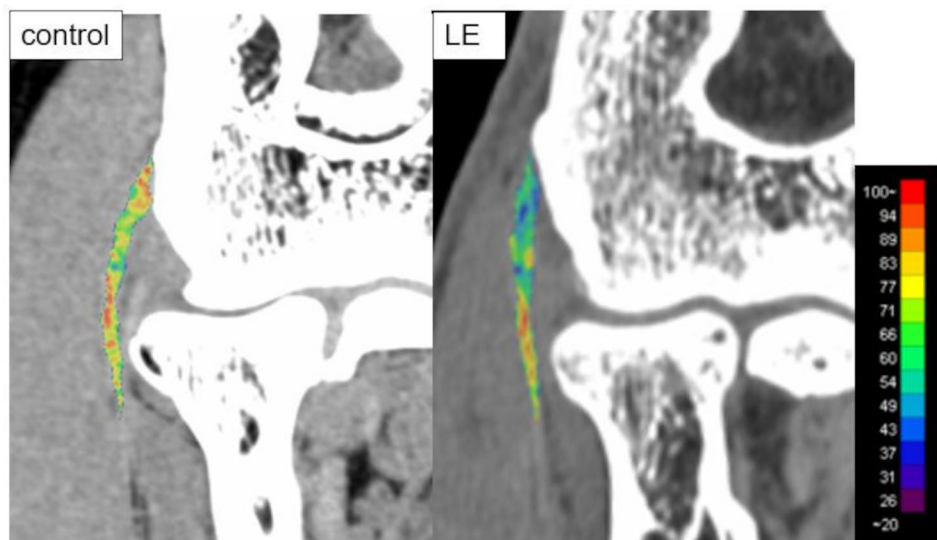


Fig. 2 HU value map of the ECRB tendon. Figure 2 shows the HU value maps with a spectrum color scale corresponding to the HU values. A quantitative comparison between the LE and control groups demonstrated lower HU values in the proximal and middle regions in the LE group

EZR17 (The Comprehensive R Archive Network, Jichi Medical University, Tochigi, Japan), an adapted version of R commander created to include commonly employed statistical functions in biostatistics.

Results

The LE and control groups comprised of 24 and 25 patients, respectively. The control group included three cases of imaging for close examination of numbness, six cases of tumors on the distal forearm or proximal upper arm far from the lateral elbow, six cases of imaging on the healthy side for surgical planning, two cases of fractures at the distal forearm or proximal humerus, three cases of early osteoarthritis, three cases of aneurysm or peripheral vascular injury, one case of medial elbow pain, and one case after ulnar shortening osteotomy. None of the patients reported any pain in the lateral elbow during imaging or in the past. For the control group, non-contrast CT scans taken before contrast administration were

used for analysis, even in cases where contrast-enhanced imaging was performed for vascular evaluation. Demographic data of the LE and control groups are presented (Table 1). There were no significant differences in age, sex, side, or BMI between the LE and control groups. The mean duration from disease onset to surgery in the LE group was 10.3 months. All the patients had a history of steroid injections. None of the patients received injections within three months of surgery or imaging studies. CT and MRI were performed within three months of surgery in all cases.

Quantitative comparison of the HU value maps showed that the LE group had lower HU values proximal to the middle region (Fig. 2). The mean HU values for the proximal region were 65.4 HU in the control group and 49.7 HU in the LE group ($P<.0001$). The mean HU values for the middle region were 67.1 HU in the control group and 58.9 HU in the LE group, showing a significant difference ($P=0.024$). The mean HU values for the distal region

were 70.8 HU in the control group and 66.1 HU in the LE group, albeit with a nonsignificant difference ($P=0.192$) (Fig. 3). In the LE group, HU values decreased significantly toward the proximal region, whereas no significant differences were observed between regions in the control group (Fig. 4). The inter-observer reliability of HU measurements showed excellent agreement with an ICC of 0.812 (95% confidence interval: 0.775–0.844).

The mean HU values for the proximal region and MRI evaluation of the ECRB tendon in LE showed a moderately negative correlation (Spearman $\rho = -0.517$, $P = 0.020$) (Fig. 5). Histological evaluation revealed that 12 (50.0%) and 12 (50.0%) patients in the LE group had grades 3 and 2 for the proximal region, respectively; 4 (16.7%), 8 (33.3%), and 12 (50.0%) patients had grades 3, 2, and 1 for the middle region, respectively; and 7 (29.2%) and 17 (70.8%) patients had grades 2 and 1 for the distal region, respectively (Fig. 6A). The mean HU values for the ECRB tendon showed a strong negative correlation with histological findings in LE (Spearman $\rho = -0.612$, $P < .0001$) (Fig. 6B).

Discussion

There is limited literature on the usefulness of HU values in evaluating the ECRB tendon in LE. This study revealed that HU values at the ECRB tendon attachment correlated with histological findings and MRI evaluations, reflecting the degree of degeneration. In the LE group, HU values were lower toward the proximal region and were significantly lower than those in the control group. Previous studies have reported that HU values decrease due to degeneration in tendons and ligaments, such as

the posterior cruciate ligament of the knee [16], the deltoid ligament of the ankle [17], and the Achilles tendon [15]. Similarly, HU values can serve as an objective and quantitative method for evaluating soft tissue degeneration in LE and may aid in predicting tissue properties.

Tendons are mostly composed of collagen and water [23]. Changes in HU values reflect alterations in the collagen/water ratio of the tendon. In LE, collagen degeneration and microtears occur with fibroblast proliferation [4]. We hypothesized that the HU values were lowered because of a higher water content than that of the normal tendon due to loosening of the matrix composition and further rupture due to degeneration. Lower HU values in the proximal areas could reflect these histological changes. Despite the significant differences observed in the proximal region, as shown in Fig. 3, some overlap in HU values was observed between the control and LE groups. This overlap likely occurs due to individual variations in tendon HU values and because the difference in HU values between normal and degenerated tendons is relatively modest, unlike dramatic changes such as an over 50% reduction. These findings suggest that for clinical applications, comparing HU values between regions within individual cases might be more valuable than establishing absolute cut-off values from population-based studies.

MRI reveals hyperintense changes on T2-weighted images and is helpful for diagnosing LE. The MRI evaluation of LE has been reported to correlate well with histological findings [24, 25]. It has also been reported that the severity of MRI signal changes correlates with the clinical score on high-resolution MRI at 3.0 Tesla [7]. In

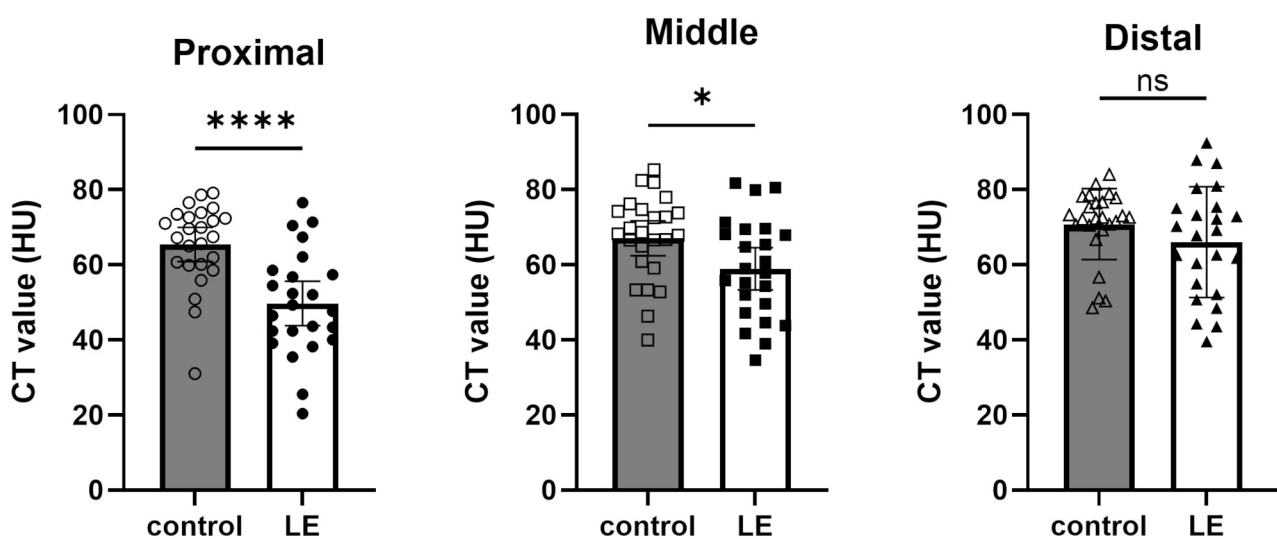


Fig. 3 Comparison of HU values in each region between the LE and control groups. The Beeswarm plot presents the HU values for the ECRB tendon in the control and LE groups. The proximal values are represented as circles, the middle values as squares, and the distal values as triangles. The control group was depicted with open markers, whereas the LE group was shown with filled markers. The means (bars) and 95% confidence intervals (error bars) are shown. Mann-Whitney U test, ns = not significant, $*P < .05$, $****P < .0001$

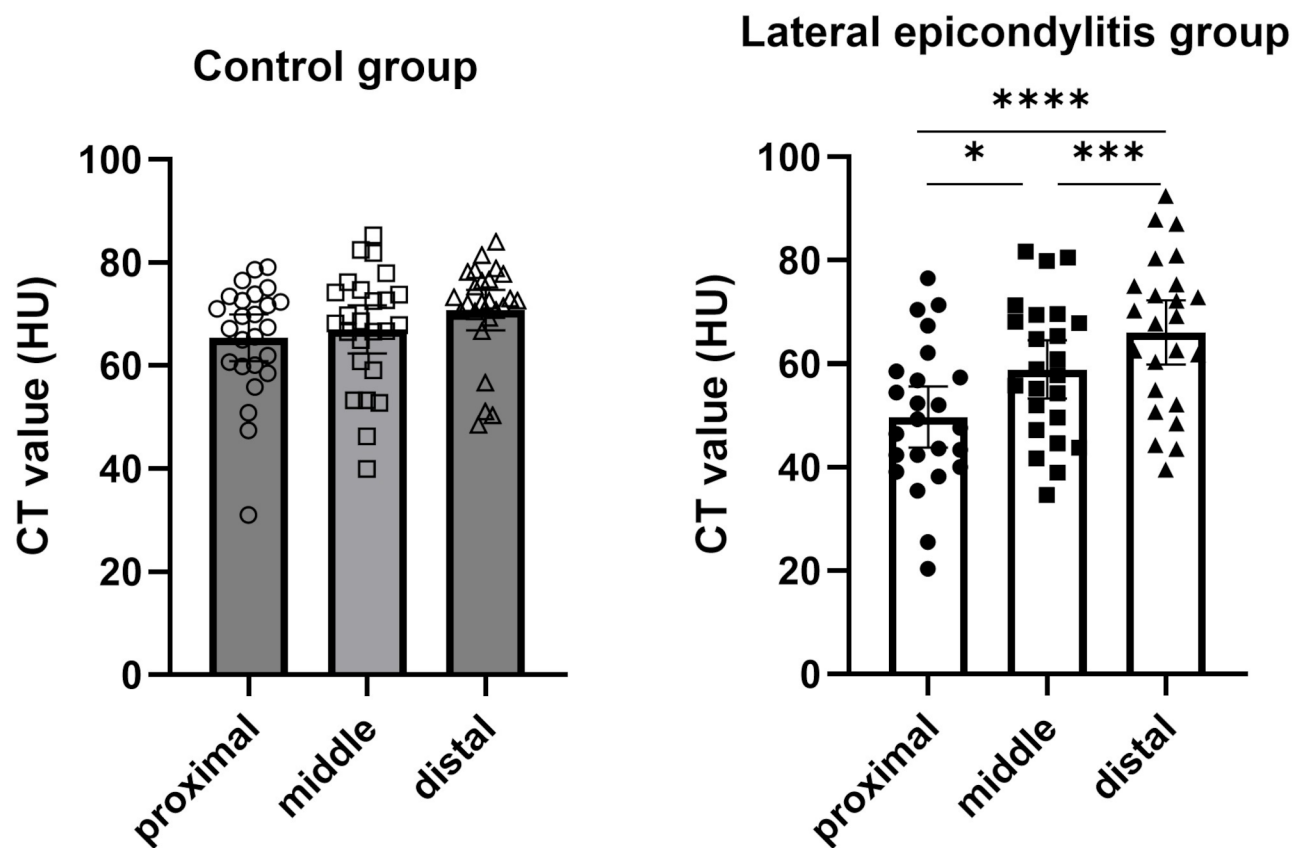


Fig. 4 Comparison of HU values between regions. The Beeswarm plot presents the HU values for the ECRB tendon in each region in the control and LE groups. The means (bars) and 95% confidence intervals (error bars) are shown. Steel-Dwass test, * $P < .05$, *** $P < .001$, **** $P < .0001$

our study, the HU values correlated well with the MRI evaluation and histological findings. A previous systematic review found T2 hyperintensities in 90% of patients with LE, while 14% of healthy controls and 50% of healthy (asymptomatic) patients with LE had increased brightness [26]. Therefore, we decided to use CT images with a healthy lateral elbow as the control group instead of the HU values of the healthy side of the same patient.

This study had several limitations. First, the small sample size is a notable limitation. Further studies with larger sample sizes are needed to determine the cutoff values. Second, technical limitations exist in the measurement of HU values because CT images require reconstruction to evaluate the ECRB tendon. Third, while intra-observer reliability was assessed, inter-observer reliability was not evaluated, which could have affected the reproducibility of our findings. Fourth, the study focused on severe cases of LE requiring surgery; therefore, further research including mild cases of LE is necessary. Fifth, the HU values were evaluated as absolute values of the mean area. In CT of the thorax and abdomen, the HU values of the aorta can be used to adjust the HU values for each tissue. However, in CT of the elbow joint, there is no suitable surrounding tissue for use as a reference. HU values

are influenced by the patients' body size, weight, position in the scanner, and differences in spectral energy [27]. The same CT scanner and body positions were used at our hospital. There were no significant differences in the BMI, and the measurement of HU values in this study was appropriate. In the control group, fractures at distant sites, bone, or soft tissue tumors may have affected the properties of the ECRB tendon. Nevertheless, considering the radiation exposure, the most suitable group was selected, as it would be ethically challenging to have healthy individuals undergo CT.

Conclusion

Our study demonstrated that degenerative changes in the ECRB tendon in LE can be quantitatively evaluated using HU measurements. Along with conventional imaging studies, such as MRI and ultrasound, detailed assessment of the ECRB tendon using HU values may provide useful information regarding the degree of tendon pathology.

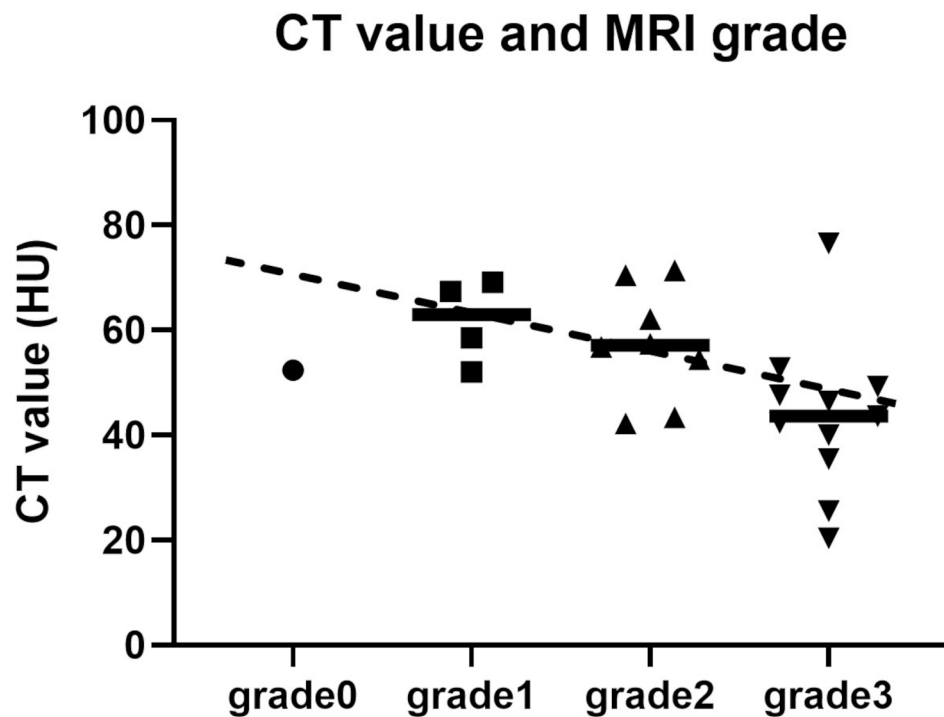


Fig. 5 MRI evaluation. The Beeswarm plot presents the HU values for the ECRB tendon in each grade divided based on the findings of ECRB tendon degeneration on MRI. The mean value (black line) is shown. Spearman's nonparametric correlation coefficient ($\rho = -0.517, P = 0.002$)

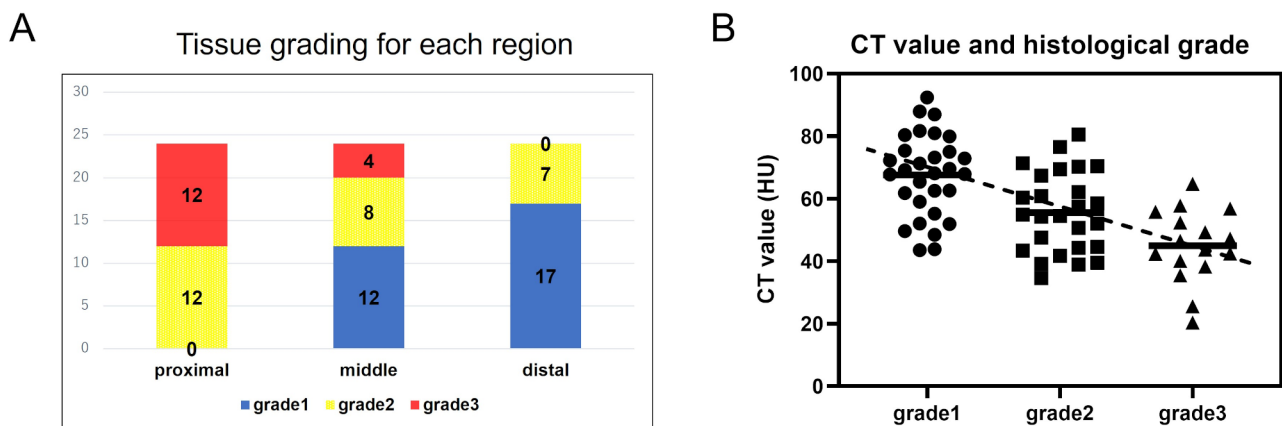


Fig. 6 Histological evaluation. (A) Tissue grading for each region: grade 1 (blue), grade 2 (yellow), and grade 3 (red). (B) The Beeswarm plot presents the HU values for each grade of the ECRB tendon divided based on the findings of ECRB tendon degeneration on histologic evaluation. The mean value (black line) is shown. Spearman's nonparametric correlation coefficient (Spearman $\rho = -0.612, P < .0001$)

Abbreviations

- LE Lateral epicondylitis
- ECRB Extensor carpi radialis brevis
- MRI Magnetic resonance imaging
- CT Computed tomography
- HU Hounsfield unit
- CET Common extensor tendon
- BMI Body mass index

Acknowledgements

Not applicable.

Author contributions

S.I. wrote the manuscript, analyzed the MRI data, and supervised all data collection; A.K. designed the overall study, performed the surgery, and proofread the manuscript; M.Y. prepared tissue sections and analyzed the data; K.Y. analyzed the CT data; R.S. and N.A. proofread the manuscript and supervised the study. All authors read and approved the final manuscript.

Funding

Not funded.

Data availability

The datasets used and/or analyzed during the current study are available from the corresponding author upon reasonable request. All data generated or analyzed during this study are plotted graphically.

Declarations

Conflict of interest

The authors declare no potential conflicts of interest regarding this manuscript.

Ethical approval

declaration Ethical approval to report this case was obtained from the Ethics Committee of Hiroshima University (No. E2022-0252).

Consent for publication

Not applicable.

Author details

¹Department of Orthopaedic Surgery, Graduate School of Biomedical and Health Sciences, Hiroshima University, Kasumi 1-2-3, Minami-Ku, Hiroshima 734-8551, Japan

²Division of Regenerative Medicine for Musculoskeletal System Medical Center for Translational and Clinical Research, Hiroshima University Hospital, Hiroshima, Japan

³Division of Diagnostic Imaging, Department of Clinical Practice and Support, Hiroshima University Hospital, Hiroshima, Japan

⁴Department of Musculoskeletal Traumatology and Reconstructive Surgery, Graduate School of Biomedical and Health Sciences, Hiroshima University, Hiroshima, Japan

Received: 4 September 2023 / Accepted: 23 January 2025

Published online: 16 April 2025

References

1. Calfee RP, Patel A, DaSilva MF, Akelman E. Management of lateral epicondylitis: current concepts. *J Am Acad Orthop Surg*. 2008;16:19–29.
2. Walz DM, Newman JS, Konin GP, Ross G. Epicondylitis: pathogenesis, imaging, and treatment. *Radiographics*. 2010;30:167–84.
3. Chourasia AO, Buhr KA, Rabago DP, Kijowski R, Lee KS, Ryan MP, et al. Relationships between biomechanics, tendon pathology, and function in individuals with lateral epicondylitis. *J Orthop Sports Phys Ther*. 2013;43:368–78.
4. Connell D, Burke F, Coombes P, McNealy S, Freeman D, Pryde D, et al. Sonographic examination of lateral epicondylitis. *AJR Am J Roentgenol*. 2001;176:777–82.
5. Coombes BK, Bisset L, Vicenzino B. A new integrative model of lateral epicondylalgia. *Br J Sports Med*. 2009;43:252–8.
6. Martin CE, Schweitzer ME. MR imaging of epicondylitis. *Skeletal Radiol*. 1998;27:133–8.
7. Qi L, Zhang YD, Yu RB, Shi HB. Magnetic resonance imaging of patients with chronic lateral epicondylitis: is there a relationship between magnetic resonance imaging abnormalities of the common extensor tendon and the patient's clinical symptom? *Med (Baltim)*. 2016;95:e2681.
8. Savnik A, Jensen B, Nørregaard J, Egund N, Danneskiold-Samsøe B, Bliddal H. Magnetic resonance imaging in the evaluation of treatment response of lateral epicondylitis of the elbow. *Eur Radiol*. 2004;14:964–9.
9. Walton MJ, Mackie K, Fallon M, Butler R, Breidahl W, Zheng MH, et al. The reliability and validity of magnetic resonance imaging in the assessment of chronic lateral epicondylitis. *J Hand Surg Am*. 2011;36:475–9.
10. Okuda M, Kobayashi S, Toyooka K, Yoshimizu R, Nakase J, Hayashi H, et al. Quantitative differentiation of tendon and ligament using magnetic resonance imaging ultrashort echo time T2* mapping of normal knee joint. *Acta Radiol*. 2022;63(11):1489–96.
11. Hounsfield GN. Nobel Award address. Computed medical imaging. *Med Phys*. 1980;7:283–90.
12. Mühl-Benninghaus R, Dressler J, Haußmann A, Simgen A, Reith W, Yilmaz U. Utility of Hounsfield unit in the diagnosis of tandem occlusion in acute ischemic stroke. *Neurol Sci*. 2021;42:2391–6.
13. Hamer OW, Aguirre DA, Casola G, Lavine JE, Woencckhaus M, Sirlin CB. Fatty liver: imaging patterns and pitfalls. *Radiographics*. 2006;26:1637–53.
14. Aubrey J, Esfandiari N, Baracos VE, Buteau FA, Frenette J, Putman CT, et al. Measurement of skeletal muscle radiation attenuation and basis of its biological variation. *Acta Physiol (Oxf)*. 2014;210:489–97.
15. Schepull T, Aspenberg P. Healing of human Achilles tendon ruptures: radiodensity reflects mechanical properties. *Knee Surg Sports Traumatol Arthrosc*. 2015;23:884–9.
16. Sumida Y, Nakasa T, Ishikawa M, Nakamae A, Adachi N. The evaluation of degeneration of posterior cruciate ligament using CT hounsfield unit in knee osteoarthritis. *BMC Musculoskelet Disord*. 2021;22:309.
17. Ikuta Y, Nakasa T, Sumii J, Nekomoto A, Adachi N. Quantitative analysis of deltoid ligament degradation in patients with chronic ankle instability using computed tomographic images. *Foot Ankle Int*. 2021;42:952–8.
18. Nimura A, Fujishiro H, Wakabayashi Y, Imatani J, Sugaya H, Akita K. Joint capsule attachment to the extensor carpi radialis brevis origin: an anatomical study with possible implications regarding the etiology of lateral epicondylitis. *J Hand Surg Am*. 2014;39:219–25.
19. Jeon JY, Lee MH, Jeon IH, Chung HW, Lee SH, Shin MJ. Lateral epicondylitis: associations of MR imaging and clinical assessments with treatment options in patients receiving conservative and arthroscopic managements. *Eur Radiol*. 2018;28:972–81.
20. Qi L, Zhu ZF, Li F, Wang RF. MR imaging of patients with lateral epicondylitis of the elbow: is the common extensor tendon an isolated lesion? *PLoS ONE*. 2013;8:e79498.
21. Nirschl RP, Pettrone FA. Tennis elbow. The surgical treatment of lateral epicondylitis. *J Bone Joint Surg Am*. 1979;61:832–9.
22. Klausner AS, Pamminer M, Halpern EJ, Abd Elah MMH, Moriggl B, Taljanovic MS, et al. Extensor tendinopathy of the elbow assessed with sonoelastography: histologic correlation. *Eur Radiol*. 2017;27:3460–6.
23. Kjaer M. Role of extracellular matrix in adaptation of tendon and skeletal muscle to mechanical loading. *Physiol Rev*. 2004;84:649–98.
24. Potter HG, Hannafin JA, Morwessel RM, DiCarlo EF, O'Brien SJ, Altchek DW. Lateral epicondylitis: correlation of MR imaging, surgical, and histopathologic findings. *Radiology*. 1995;196:43–6.
25. Steinborn M, Heuck A, Jessel C, Bonel H, Reiser M. Magnetic resonance imaging of lateral epicondylitis of the elbow with a 0.2-T dedicated system. *Eur Radiol*. 1999;9:1376–80.
26. Pasternack I, Tuovinen EM, Lohman M, Vehmas T, Malmivaara A. MR findings in humeral epicondylitis. A systematic review. *Acta Radiol*. 2001;42:434–40.
27. Birnbaum BA, Hindman N, Lee J, Babb JS. Multi-detector row CT attenuation measurements: assessment of intra- and interscanner variability with an anthropomorphic body CT phantom. *Radiology*. 2007;242:109–19.

Publisher's note

Springer Nature remains neutral with regard to jurisdictional claims in published maps and institutional affiliations.